RSC Advances

ROYAL SOCIETY OF CHEMISTRY

www.rsc.org/advances

RSC Advances

Cite this: DOI: 10.1039/c0xx00000x

PAPER

www.rsc.org/materials

Steam Explosion-Ionic Liquid Pretreatments on Wetland Lignocellulosic Biomasses of *Phragmites* (sp.) and *Thalia dealbata* for BioH_2 Conversion

Hongyun Peng,[*a] Lingling Gao, [a] Mengjiao Li, [a] Yibin Shen, [a] Qiongqiu Qian [b] and Xia Li [a]

Received (in XXX, XXX) Xth XXXXXXXXX 20XX, Accepted Xth XXXXXXXXX 20XX

DOI: 10.1039/b000000x

BioH_2 conversion from wetland lignocellulosic biomass is one of the promising alternatives to fossil fuels. Both *Phragmites* (sp.) and *Thalia dealbata* are holocelluloses-rich and lignin-rich wetland plants for biomass. Scanning electron microscopy (SEM) and fourier transform infrared spectroscopy (FTIR) demonstrated alteration of lignocellulosic structures due to hemicelluloses removal by steam explosion (SE) pretreatment, and further disruption of cellulose crystallinity after treatment with SE followed by [Bmim]Cl (SE-[Bmim]Cl). Thermogravimetry/differential thermogravimetry (TG/DTG) displayed increase in amorphous cellulose and partially delignification in lignocellulosic structures as a consequence of SE-[Bmim]Cl. The pretreatment of both SE and SE-[Bmim]Cl led to lignocellulosic substrates with improved properties in terms of their conversion into glucose and bioH_2. Five-to-ten folds (by SE) and ten-to-twenty folds (by SE-[Bmim]Cl) glucose were released from the lignocellulosic substrates of both plants than those of contrast samples. Compared to *Phragmites* (sp.), the greater destruction in lignocellulosic structure of *Thalia dealbata* as consequences of SE and SE-[Bmim]Cl, increased the accessible surface area and disrupted the cellulose crystallinity much more thus efficient for bioH_2 conversion. The bioH_2 of 1.97±0.14 mmol H_2/g dry weight (DW) yielded after sludge anaerobic fermentation of *Thalia dealbata* treated with SE, and it increased to 4.79±0.86 mmol H_2/g DW after SE-[Bmim]Cl treatment; while for *Phragmites* (sp.) it was 1.45±0.42 and 2.75±0.76 mmol H_2/g DW after SE and SE-[Bmim]Cl pretreatment, respectively. Therefore, SE-[Bmim]Cl pretreatment can be developed for efficiently enhancing bioH_2 conversion from wetland plant *Thalia dealbata*.

Introduction

The extensive consumption of fossil fuel has created global environmental issues. Eutrophication becomes an environmental issue worldwide. Moreover, the increasingly worsening water quality induced by excessive nitrogen (N) and phosphorus (P) inputs speeds up water eutrophication. [1, 2] As an effective process for eutrophication treatment, the constructed wetland is in increasing operation to mitigate deteriorating wastewater pollutants and nutrients inputs. [3-6] However, a great number of lignocellulosic biomass are produced through wastewater treatment, which makes the constructed wetland becoming the cellulosic biofuel production system, where high productive plant species are of great potential. [7] Green reed (*Phragmites* (sp.)) is a new variety of common reed (*Phragmites australis*). Not only both *Phragmites* species have approximately three to five times greater productivities than the dedicated biofuel crops switchgrass, but also they can reduce N use, thus can be used as the preferable wetland plants. [8-10] Water arum (*Thalia dealbata*) is another high productive wetland plant for N removal from wastewater in east China. [11, 12] With more requirements on renewable energy, the increasing attention focuses on harvest of the existing strands of wetland biomass for cellulosic biofuel conversion. [13,14]

The big challenge in bioH_2 transformation from wetland biomass is the pretreatment of lignocellulosic substrates, which is strongly conditioned by bioaccessibility of cellulose. [15-17] Aim of pretreatment is to increase the accessibility of enzymes to cellulose through removing lignin and hemicelluloses components, and to reduce cellulose crystallinity in substrates. [18] Better pretreatment leading to solubilisation of celluloses is also recommended as the efficient process for bioH_2 conversion. [19, 20] So the adequate pretreatment is of great interest to fractionate the lignocelluloses better. Steam explosion (SE) pretreatment can provide effective fractionation of lignocellulosic components and generate cellulose-rich fractions through hemicelluloses degradation due to destruction of cell-wall matrix. [21, 22] Furthermore, cellulose components can be dissolved without derivatization in high concentrations of ionic liquids (ILs), thus making SE and ILs the attractive biomass pretreatments. [23-28] In addition, compared to conventional pretreatments, the

advantages of SE and ILs hold a significantly lower environmental impact and less use of hazardous chemicals.

ILs are known to dissolve cellulose by effectively disrupting the complex network of non-covalent interactions between carbohydrates and lignin in biomass. The 1-butyl-3-methyl-imidazolium chloride ([Bmim]Cl) was found to be the most effective IL capable of dissolving up to 25% (w/w) cellulose [25] due to chloride anion (Cl^-) present responsible for dissolution of cellulose. [29] Cellulose was disordered in [Bmim]Cl solution during the dissolution process as measured by high-resolution carbon-13 nuclear magnetic resonance (^{13}C NMR), where no degradation of cellulose occurred. [24, 30-32] The addition of water, alcohol or acetone as anti-solvent resulted in a precipitation of cellulose from the [Bmim]Cl solution.[33, 34] The assistance of microwave irradiation can enhance efficiency of dissolution in ILs compared to ordinary thermal treatment. [35] In addition, ILs were recovered up to 97% (w/w) of the initial mass, it can be reused after pretreatment as in viewed that the pretreatment did not alter the ^1H and ^{13}C NMR spectra of the used ILs compared to the purity of ILs before pretreatments. [36] Therefore the objectives of this study (as illustrated in Scheme 1) are : (1) to perform the pretreatment with SE and IL ([Bmim]Cl as a solvent, with microwave-assistance) on lignocellulosic substrates of both *Phragmites* (sp.) and *Thalia dealbata* in constructed wetland; (2) to characterize the compositional (cellulose, hemicelluloses, lignin) and structural features (crystallinity of cellulose, lignin, surface area and porosity) of lignocellulosic substrates through scanning electron microscopy (SEM), fourier transform infrared spectroscopy (FTIR), BET surface area and porosity, and thermogravimetry/differential thermogravimetry (TG/DTG); and (3) to evaluate enzymatic hydrolysis, sludge anaerobic fermentation and bioH_2 yield with HPLC and GC measurements.

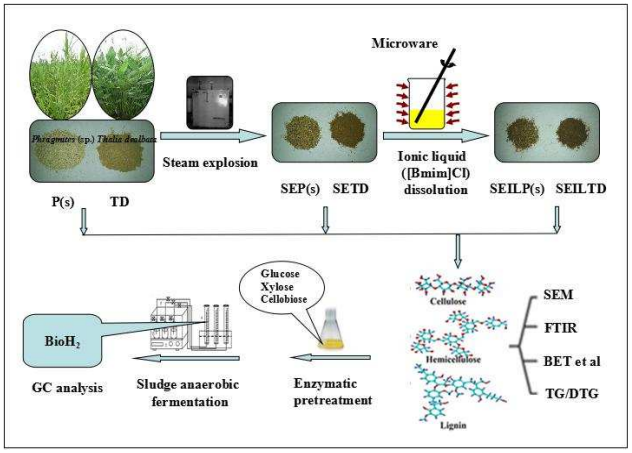

Scheme 1 The bioH_2 conversion strategies of lignocellulosic substrates of wetland plants under the pretreatments by SE and [Bmim]Cl (P(s) and TD referring to *Phragmites* (sp.) and *Thalia dealbata*, respectively; SEP(s) and SETD representing SE-pretreated *Phragmites* (sp.) and *Thalia dealbata*, respectively; SEILP(s) and SEILTD representing SE-[Bmim]Cl pretreated *Phragmites* (sp.) and *Thalia dealbata*, respectively).

Results and discussion

Chemical Composition of Wetland Lignocellulosic Biomass

Phragmites (sp.) and *Thalia dealbata* are large-biomass and fast-growth wetland plants in the subsystem of constructed wetlands located at Linan municipal wastewater treatment plant, Zhejiang Province, China. [10, 12] *Phragmites* (sp.) are planted once and can grow for many years with relatively low maintenance, while *Thalia dealbata* belongs to the annual grasses. The lignocellulosic components consist of cellulose, hemicelluloses and lignin accounting for 37-43%, 23-33% and 13-14% of the dried biomass, respectively, as listed in Table 1. *Phragmites* (sp.) stalk enriches higher contents of cellulose and hemicellulose as compared to *Thalia dealbata* stalk.

SE Pretreatment of Wetland Lignocellulosic Biomass

As seen in Fig. 2, slight increase in cellulose appeared in SE-pretreated *Phragmites* (sp.) lignocelluloses but not in SE-pretreated *Thalia dealbata* lignocelluloses than that of the raw material. Under lower steam pressure of 2.0 and 2.5 MPa, rising of residence time from 60s to 90s slightly decreased the cellulose in SE-pretreated *Phragmites* (sp.) lignocelluloses (Fig. 2a). Furthermore, no impacts on lignin removal but with slightly increased lignin appeared in SE-pretreated *Thalia dealbata* lignocelluloses (Table 1). SE-pretreatment disrupted the lignocellulosic structure through degradation of hemicellulosic components and generation of lignin-related components. These impacts were closely related to the sort of raw materials. The optimal cellulose-rich fractionation in SE-pretreated *Phragmites* (sp.) lignocelluloses yielded under steam pressure of 3.0 MPa, while for *Thalia dealbata* it was at 2.5 MPa.

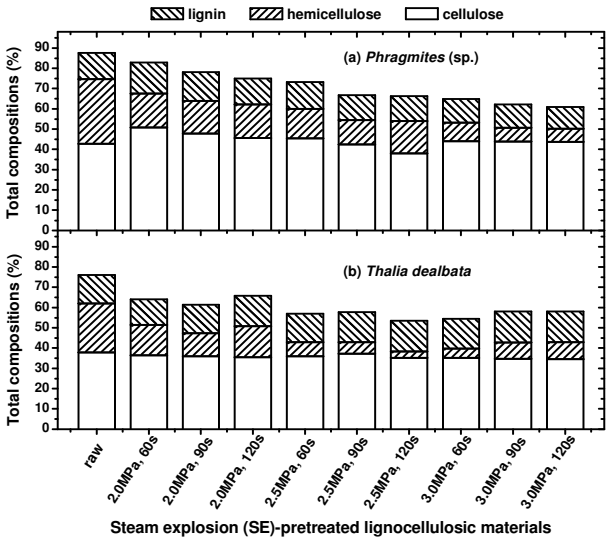

Fig. 1 Total compositions (cellulose, hemicellulose and lignin) of the SE-pretreated stalk lignocelluloses from (a) *Phragmites* (sp.) and (b) *Thalia dealbata* under different steam pressure and residence time.

The rising of steam pressure and residence time significantly reduced total lignocellulosic compositions in SE-pretreated lignocelluloses of both plants than the raw material, with hemicelluloses removal much more than cellulose and lignin (Fig. 1 and Fig. 2). Lower steam pressure caused the slight removal of

hemicelluloses, while higher steam pressure generated the significant removal of hemicelluloses from SE-pretreated lignocelluloses of both plants. The great hemicelluloses removal occurred at steam pressure of 3.0 MPa for *Phragmites* (sp.) while for *Thalia dealbata* it was at 2.5 MPa (Fig. 2, Table 1).

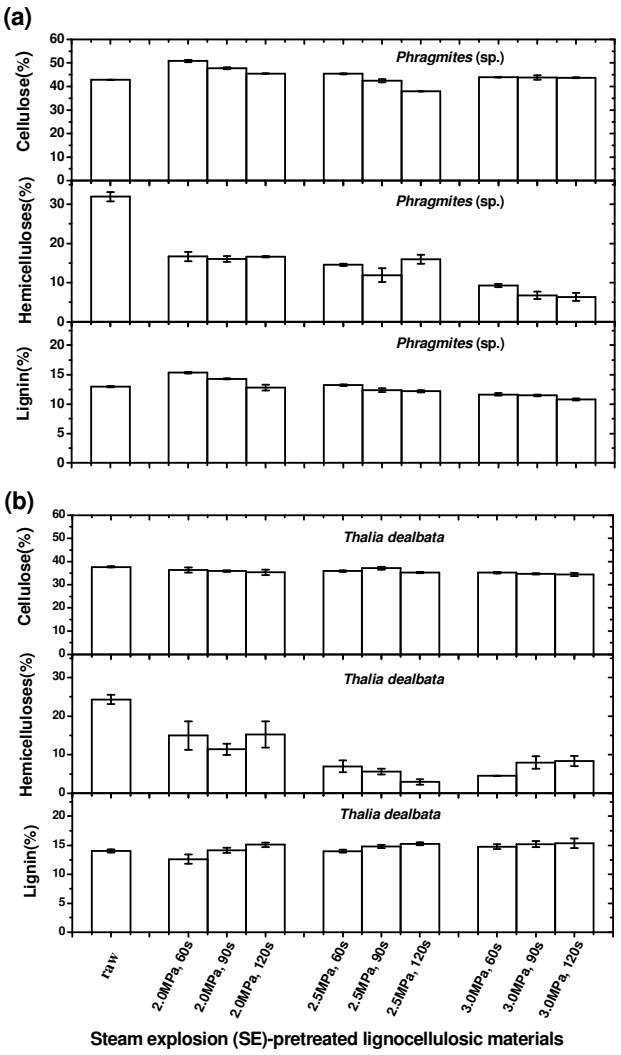

Fig. 2 Contents of cellulose, hemicelluloses and lignin of the SE-pretreated stalk lignocelluloses from (a) *Phragmites* (sp.) and (b) *Thalia dealbata* under different steam pressure and residence time.

Enzymatic Hydrolysis of SE-pretreated Lignocelluloses

The optimization of enzymatic saccharification was performed on SE-pretreated *Thalia dealbata* lignocelluloses (2.0-3.0 MPa, 90 s) as substrate. Low activities of enzymatic hydrolysis in raw material but considerably increased activities in SE-pretreated lignocelluloses yielded. The optimal enzymatic hydrolysis appeared at substrate concentration of 40 g/L (Fig. 3a), enzyme concentration of > 20 FPU/g (substrate) (Fig. 3b), pH 4.8 (Fig. 3c), 50 °C (Fig. 3d) and hydrolysis time of 24 h (Fig. 3e). Under the optimal hydrolysis conditions, the enzymatic hydrolysis rate of SE-pretreated lignocelluloses from both plants increased significantly, about ten times higher than those of the raw material (Fig. 4). Enzymatic hydrolysis highly depended on the nature of lignocellulosic substrates and SE-pretreated conditions. The rising of steam pressure and residence time presented the increased trends in enzymatic hydrolysis rate of SE-pretreated lignocelluloses, with that of *Thalia dealbata* increased faster than *Phragmites* (sp.). Compared to *Phragmites* (sp.), lignocellulosic components of *Thalia dealbata* were affected much more by SE pretreatment, facilitating the accessibility of cellulose in substrate. Enzymatic hydrolysis rate was around 61.3% for *Thalia dealbata* under 2.5 MPa, while it was 62.9% under high steam pressure of 3.0 MPa for *Phragmites* (sp.) (Fig. 4).

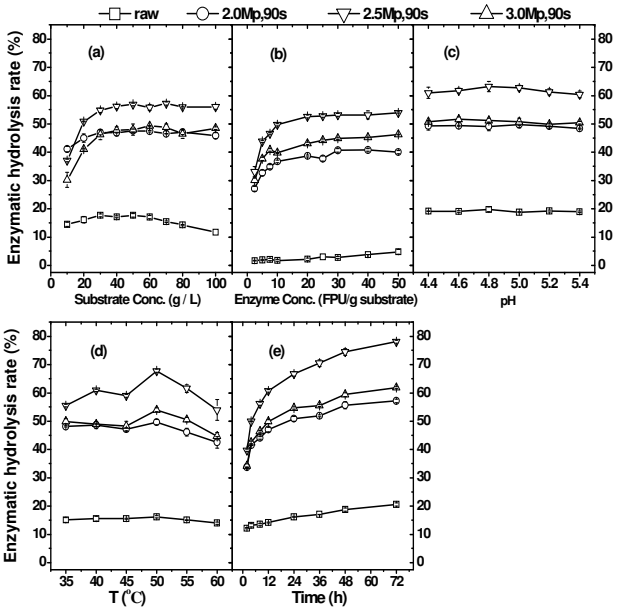

Fig. 3 Optimization of saccharification reaction for SE-fractioned stalks lignocelluloses from *Thalia dealbata*. (a) Enzyme concentration (g/L); (b) Substrate concentration (FPU/g substrate); (c) pH; (d) Hydrolysis temperature (°C); (e) Hydrolysis time (h).

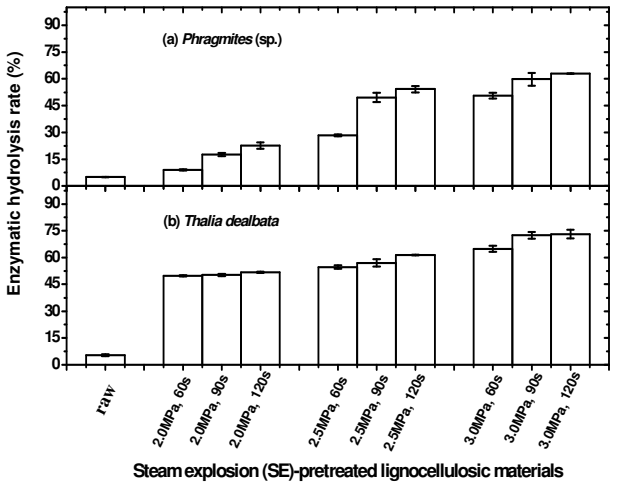

Fig. 4 Enzymatic hydrolysis rates of SE-pretreated lignocelluloses from (a) *Phragmites* (sp.) and (b) *Thalia dealbata* under different steam pressure and residence time.

[Bmim]Cl Dissolution of SE-pretreated Lignocelluloses

Lignocellulosic substrates present compositional and structural features limiting their accessibility of celluloses for bioH_2 conversion. In this study, the optimization of microwave-assistant solubilisation in IL ([Bmim]Cl as solvent) was developed by using SE-pretreated *Phragmites* (sp.) lignocelluloses (3.0 MPa, 90 s) as substrate. This solubilisation in [Bmim]Cl depended on the nature of lignocellulosic materials and microwave conditions (microwave time, microwave power, and initial concentration of lignocelluloses in [Bmim]Cl). The optimal microwave-assisted [Bmim]Cl dissolution conditions were 400W, 40s and a 1/20 ratio of SE-pretreated lignocelluloses in [Bmim]Cl (Fig. 5), by which cellulose can be regenerated from [Bmim]Cl solution through addition of sufficient de-ionized water as anti-solvents. Therefore SE-pretreated *Phragmites* (sp.) lignocelluloses (3.0 MPa) and *Thalia dealbata* lignocelluloses (2.5 MPa) performed optimal microwave assisted-[Bmim]Cl treatment. As seen in Table 1, the slightly decreased hemicellulose and lignin appeared in [Bmim]Cl-regenerated *Phragmites* (3.0 MPa, 90 s) and *Thalia dealbata* (2.5 MPa, 90 s) lignocelluloses. Moreover, slightly enhanced cellulose appeared in [Bmim]Cl-regenerated *Phragmites* (sp.) lignocelluloses, [37] however the significant changes in lignocellulosic structures may occur.

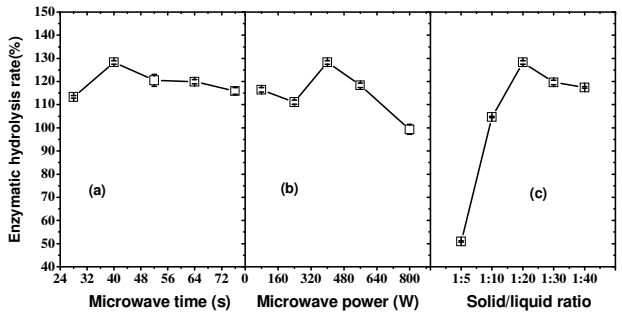

Fig. 5 Optimization of microwave assisted-[Bmim]Cl dissolution of SE-pretreated *Phragmites* (sp.) lignocelluloses (3.0 MPa, 90 s) (a. Microwave time; b. Microwave power; c. Solid/liquid ratio of lignocelluloses in [Bmim]Cl).

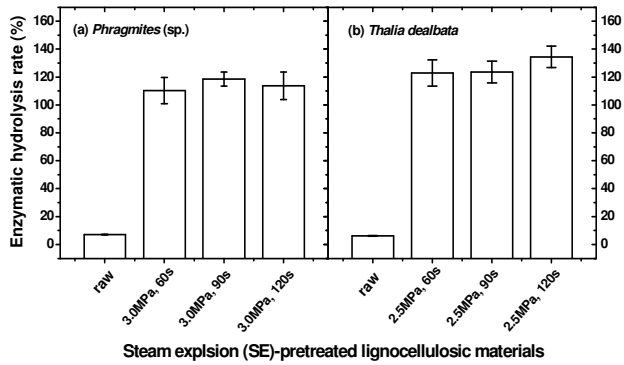

Fig. 6 Enzymatic hydrolysis rates of [Bmim]Cl-regenerated lignocelluloses from (a) SE-pretreated *Phragmites* (sp.) and (b) SE-pretreated *Thalia dealbata* under different steam pressure and residence time.

Table 1. Cellulose, hemicelluloses and lignin in lignocellulosic substrates

Sample	Cellulose (%)	Hemicellulose (%)	Lignin (%)
Water arum (*Thalia dealbata*)			
raw	37.7±0.3	24.3±1.2	14.0±0.3
SE-pretreated (2.5MPa)	37.2±0.6	5.7±0.8	14.8±0.3
[Bmim]Cl-regenerated (2.5MPa)	37.1±0.1	5.4±0.2	14.6±0.1
Green reed (*Phragmites* (sp.))			
raw	42.8±0.1	31.9±1.2	13.0±0.1
SE-pretreated (3.0MPa)	43.9±0.9	6.8±1.0	11.5±0.1
[Bmim]Cl-regenerated (3.0MPa)	45.0±0.2	6.0±0.2	11.3±0.2

The raw material untreated with SE (Fig. 4) and then followed by microwave assisted-[Bmim]Cl treatment (Fig. 6) presented pretty low enzymatic hydrolysis rate at around 9%. To the contrary, a significant increase in enzymatic hydrolysis rate yielded in [Bmim]Cl-regenerated lignocelluloses of both plants. As compared to SE-pretreated material (Fig. 4), SE-[Bmim]Cl treatment led to 2 times enzymatic hydrolysis rate increase, reaching 110% and 130% of regenerated *Phragmites* (sp.) and *Thalia dealbata* lignocelluloses, respectively (Fig. 6). That meant all celluloses plus a part of hemicelluloses were hydrolyzed from [Bmim]Cl-regenerated lignocelluloses, resulting in ten-to-twenty-fold glucose released in hydrolysates. While cellulose partially hydrolyzed from SE-pretreated lignocelluloses, as evident by five-to-ten-fold glucose increased in hydrolysates (Table 2). The hydrolytic enzymes worked most efficiently for cellulose and less for hemicellulose, so that the enzymatic saccharification byproducts in the hydrolysates were mainly glucose with less xylose and cellobiose (Table 2).

Table 2. Sugars in enzymatic hydrolysates of lignocellulosic substrates

Sample	Glucose % (w/w biomass)	Xylose % (w/w biomass)	Cellobiose % (w/w biomass)
Thalia dealbata			
raw	7.81 ±0.22	2.68±0.25	NR
SE-pretreated (2.5MPa)	38.65±7.49	0.38±0.19	NR
[Bmim]Cl-regenerated (2.5MPa)	72.11±0.20	0.62±0.15	2.59±0.22
Phragmites (sp.)			
raw	4.54±0.43	NR	NR
SE-pretreated (3.0MPa)	35.33±0.96	2.19±0.16	NR
[Bmim]Cl-regenerated (3.0MPa)	88.80±0.23	1.27±0.03	3.17±0.12

NR: No detected results.

Differences observed only by SE and SE-[Bmim]Cl pretreatments could be due to their significant difference on degradation process of substrates. Treatment with SE-[Bmim]Cl can depolymerize cellulose more efficiently through disrupting the intr- and inter- hydrogen bonds of cellulose molecules, resulting in the fragmental cellulosic materials with highly

amorphous structure. [34] Thus better enzyme accessibility was achieved with the significantly accelerated enzymatic hydrolysis rate and high production of reducing sugar from [Bmim]Cl-regenerated materials. [38]

$BioH_2$ Fermentation

Thermophilic fermentation of lignocelluloses remained very slow or inhibited in general, [39] as evident by the low $bioH_2$ yield at 1.22 - 1.26 mmol H_2/g dried weight (DW) of raw materials (Table 3). After SE pretreatment, $bioH_2$ of 1.45 - 1.97 mmol H_2/g DW was produced in lignocelluloses of both plants and it was increased to 2.75 - 4.79 mmol H_2/g DW after SE-[Bmim]Cl treatment (Table 3).

Fig. 7 summarized material balance for pretreatment, saccharification and fermentation of both *Thalia dealbata* and *Phragmites* (sp.) in two scenarios (also illustrated in Scheme 1): (a) SE pretreatment and (b) SE-[Bmim]Cl pretreatment. On the basis of 100 g of plant biomass, the majority of hemicelluloses degraded, producing cellulose-rich lignocelluloses after SE pretreatment, and enhancing $bioH_2$ yield after saccharification and fermentation (Table 1 and Fig. 7a). As compared to SE-pretreated samples, SE-[Bmim]Cl pretreatment on these cellulose-rich lignocellulosic structures resulted in enhanced $bioH_2$ yield by above 2-fold (Table 3 and Fig. 7b), which could be attributed to 2-fold enhancements in both enzymatic hydrolysis rate and glucose released from [Bmim]Cl-regenerated lignocelluloses (Fig. 4 and Fig. 6, Table 2). SE-[Bmim]Cl pretreatment facilitated efficiently transformation of cellulose in substrate into soluble polysaccharide monomer sugars (i.e., glucose) with higher yield, causing a positive effect on $bioH_2$ conversion (Table 2 and Table 3, Fig. 7b).

Table 3. Thermophilic fermentation of lignocellulosic substrates for 48 h $BioH_2$ conversion

Sample	$BioH_2$ (mmol H_2/g DW)
Thalia dealbata	
raw	1.22±0.25
SE-pretreated (2.5MPa)	1.97±0.14
[Bmim]Cl-regenerated (2.5MPa)	4.79±0.86
Phragmites (sp.)	
raw	1.26±0.08
SE-pretreated (3.0MPa)	1.45±0.42
[Bmim]Cl-regenerated (3.0MPa)	2.75±0.76

After SE-[Bmim]Cl treatment, $bioH_2$ yield converted from annual grasses *Thalia dealbata* was much higher than that from corn or rice straw. [14] However the comparatively lower $bioH_2$ yield of 2.75±0.76 mmol H_2/g DW was converted from *Phragmites* (sp.) (Table 3). The utilization mechanism of lignocelluloses could be different between *Thalia dealbata* and *Phragmites* (sp.). The lignocellulosic structures of *Phragmites* (sp.) exhibited more resistant to deconstruction than annual grasses *Thalia dealbata*. Therefore it need further elucidation of pretreatment by SE and SE-[Bmim]Cl on compositional and structural features of lignocelluloses during $bioH_2$ conversion.

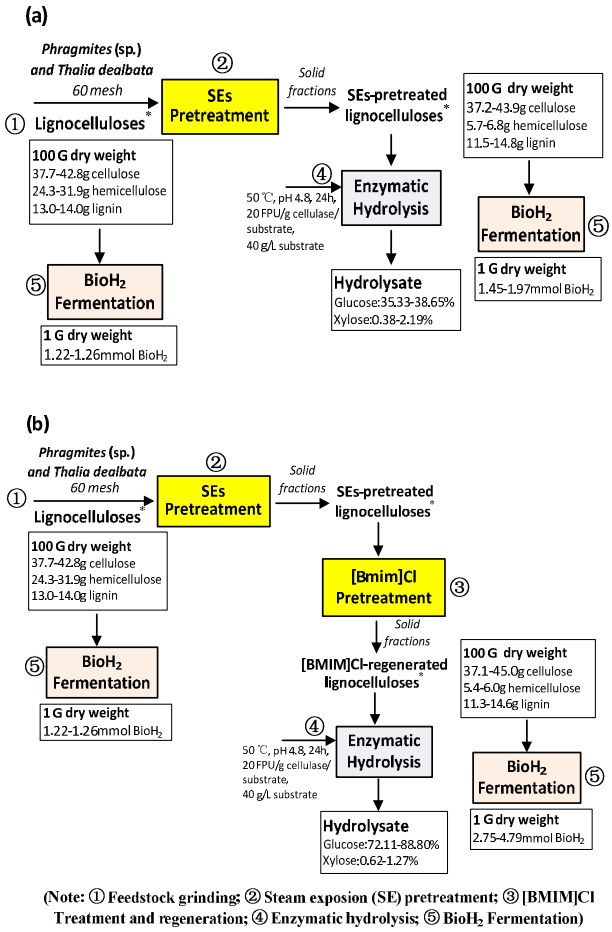

Fig. 7 Material balance on proposed pretreatments (a. SE, b. SE-[Bmim]Cl), saccharification and fermentation processes.

Structure and Crystallinity Assessment of Lignocelluloses

The major obstacle in utilizing wetland lignocelluloses as fermentation substrates is recalcitrance of biomass itself. Both *Phragmites* (sp.) and *Thalia dealbata* enrich cellulose and hemicellulose as main lignocellulosic components but characteristic with different lignocellulosic structures affecting their enzymatic hydrolysis, anaerobic fermentation as well as $bioH_2$ yield. The pretreatments on factors affecting the structural features such as crystallinity of cellulose, accessible surface area and lignin in lignocellulosic substrates were discussed.

SEM images. The intact plant cell wall presented typical vascular bundles and fibril structures in raw *Thalia dealbata* and *Phragmites* (sp.) stalks. *Thalia dealbata* possess the loose structures while *Phragmites* (sp.) holds the dense and long vascular bundles structures (Fig. 8A and Fig. 8D). SE pretreatment greatly impacted vascular structures of *Thalia dealbata* lignocelluloses compared to *Phragmites* (sp.), while no destruction of crystal structures occurred for both plants. After SE-[Bmim]Cl pretreatment, lignocellulosic structures were significantly changed, giving rise to conglomerate textures (Fig. 8C and Fig. 8F). Furthermore, some irregular cracks appeared on the surface of [Bmim]Cl regenerated materials (Fig. 8C and Fig. 8F) compared to the raw material. SE-[Bmim]Cl pretreatment

altered lignocellulosic structure and these alterations were probably attributed to the destroyed crystalline cellulose during its dissolution into [Bmim]Cl solution, leaving a highly homogeneous morphology on regenerated materials from [Bmim]Cl solution.

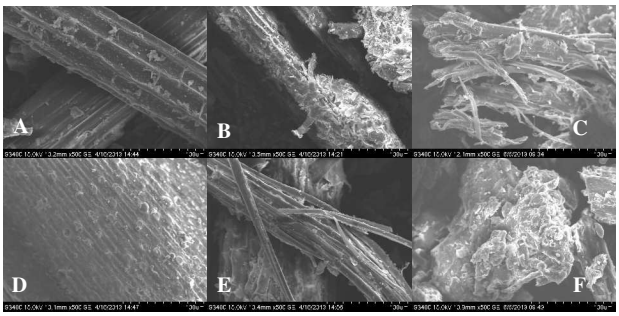

Fig. 8 SEM images of raw and pretreated lignocellulosic materials. A, B and C representing the raw, SE-pretreated and [Bmim]Cl-regenerated *Thalia dealbata* (2.5MPa, 90s), respectively; D, E and F representing the raw, SE-pretreated and [Bmim]Cl-regenerated *Phragmites* (sp.) (3.0MPa, 90s), respectively. All images were taken at same scale (×500).

Table 4. Accessible surface area and pore volume of lignocelluloses

Parameters	raw	SE-pretreated
	Thalia dealbata	
BET surface area (m^2/g)	1.47	2.81
Langmuir surface area (m^2/g)	2.46	5.04
BJH adsorption cumulative surface area of pores (m^2/g)	1.57	2.78
BJH adsorption cumulative volume of pores ($\times10^{-3}$ cm^3/g)	5.14	9.36
BJH adsorption average pore diameter (nm)	131.13	134.75
	Phragmites (sp.)	
BET surface area(m^2/g)	0.70	0.50
Langmuir surface area (m^2/g)	0.95	0.65
BJH adsorption cumulative surface area of pores (m^2/g)	0.27	0.27
BJH adsorption cumulative volume of pores ($\times10^{-3}$ cm^3/g)	3.49	5.21
BJH adsorption average pore diameter (nm)	524.35	784.97

Accessible Surface Area and Porosity Analyses. Parameters such as accessible surface area and pore volume have been shown to affect the bio-digestibility of lignocellulosic substrates. Compared to the raw material, SE pretreatment effectively enhanced surface area (BET and Langmiur) in *Thalia dealbata* lignocelluloses, but slightly decreased surface area appeared in *Phragmites* (sp.) lignocelluloses (Table 4). SE pretrearment much more impacted lignocelluloses on *Thalia dealbata* than on *Phragmites* (sp.), which is consistent with SEM images (Fig. 6D and Fig. 6E). In addition, both BJH adsorption cumulative volumes and pore diameters increased significantly from both plants after SE pretreatment (Table 4). The raw and SE-pretreated *Thalia dealbata* lignocelluloses hold greater surface area (BET and Langmiur) and pore volume of cellulose compared to *Phragmites* (sp.), facilitating its bio-digestibility for enzymatic attack in the subsequent hydrolysis process and bioH_2 conversion. After SE-[Bmim]Cl treatment, the regenerated materials from [Bmim]Cl solution were fragmental cellulosic materials with highly amorphous structure beneficial for bioH_2 conversion.

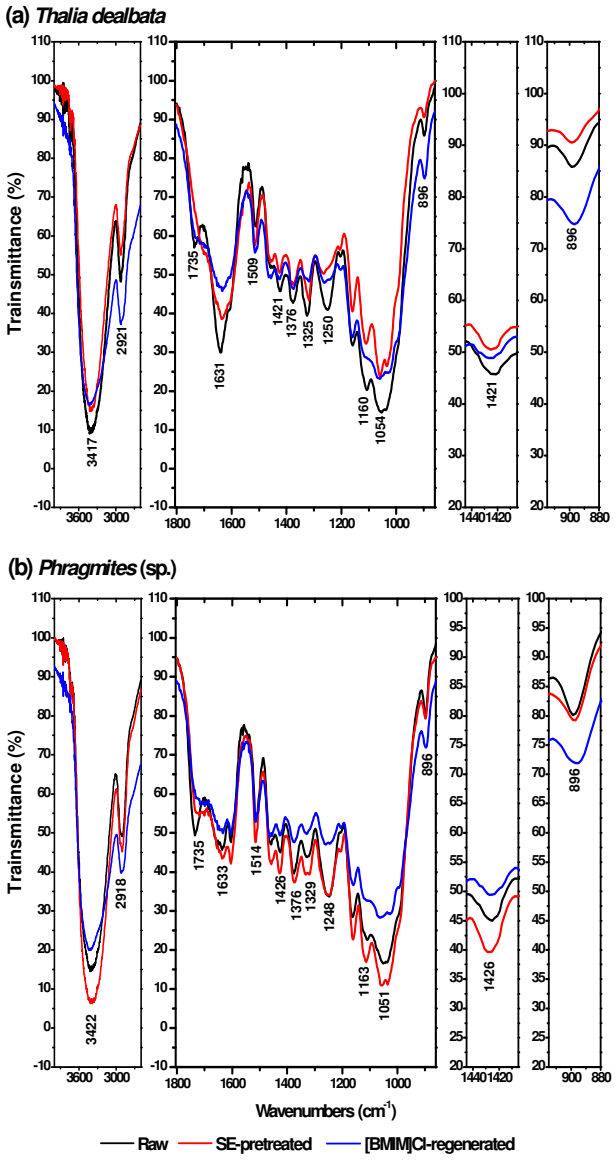

Fig. 9 FTIR spectrum of (a) *Thalia dealbata* (raw, SE-pretreated and [Bmim]Cl-regenerated *Thalia dealbata* (2.5MPa, 90s)) and (b) *Phragmites* (sp.) (raw, SE-pretreated and [Bmim]Cl-regenerated *Phragmites* (sp.) (3.0MPa, 90s)).

FTIR spectra. The strong band in IR spectra was representative at 3200-3600 cm^{-1} range (assigned to axial deformation of O-H group), for *Thalia dealbata* and *Phragmites* (sp.), this peak in this study appeared around 3417 (or 3422 cm^{-1}). The band at 2921 (or 2918 cm^{-1}) represented axial deformation of C-H group. The band at 1735 cm^{-1}, assigned to carbonyl group (C=O) between hemicelluloses and lignin,

strengthened in the raw materials, while they were greatly reduced by both pretreatments. In addition, the weakened peak shapes and intensities at 1250 cm^{-1} (assigned to hemicellulose) appeared after pretreatments. This could come from the significant removal of hemicelluloses by SE and SE-[Bmim]Cl treatments (Fig. 1 and Fig. 2). The band at 1631 cm^{-1}, assigned to absorbed water bending vibration, was significantly reduced by SE-[Bmim]Cl pretreatment which could be related to the decreased O-H group in substrate. The interaction between free Cl^- in [Bmim]Cl and O-H groups disrupted the hydrogen bonds present within and between the lignocellulosic substrates.

FTIR spectra at 1800-800 cm^{-1} regions were characteristic of the cellulose structure. The bands at 1421 (or 1426 cm^{-1}) and 896 cm^{-1}, assigned to CH_2 scissoring motion and C-O-C stretching in cellulose, respectively, are quite sensitive to the amount of crystalline and amorphous cellulose. [40] The infrared ratio H1421/H896 (or H1426/H896) is commonly called lateral order indice (LOI) to determine the amount of crystalline cellulose. [40, 41] Total crystallinity index (TCI), the ratio of H1376/H2918 or H1376/H2921 (CH and CH_2 stretching), is also used to study the crystallinity changes. [41, 42]

Table 5. Crystallinity indices of lignocellulosic materials before and after treatment with SE and SE-[Bmim]Cl

Substrates	LOI	TCI
Thalia dealbata		
raw	4.12	1.11
SE-pretreated (2.5MPa)	5.53	1.22
[Bmim]Cl-regenerated (2.5MPa)	2.43	0.79
Phragmites (sp.)		
raw	3.00	1.20
SE-pretreated (3.0MPa)	3.63	1.16
[Bmim]Cl-regenerated (3.0MPa)	2.34	0.80

As seen in Table 5, high values of LOI and TCI in the raw materials indicated that both *Thalia dealbata* and *Phragmites* (sp.) had high crystallinity of cellulose and ordered lignocellulosic structures before pretreatments. As compared to the raw material, pretreatment with SE dramatically increased the LOI values for both plants, while TCI values was slightly increased for *Thalia dealbata* but slightly decreased for *Phragmites* (sp.). Comparatively, SE-[Bmim]Cl treatment significantly decreased the values of both LOI and TCI for both plants. No destruction of cellulose crystallinity appeared by SE pretreatment, while the disruption of ordered lignocellulosic structures occurred by SE-[Bmim]Cl treatment. This was in good agreement with the observation from SEM images. During solubilisation in [Bmim]Cl, the cellulosic materials lost their crystalline structures and restructured themselves into mostly amorphous forms, which made structures of regenerated lignocelluloses less crystalline. Due to the disruption of ordered structure and reduction in crystallinity, SE-[Bmim]Cl pretreated materials became more susceptible to enzymatic attack in the subsequent hydrolysis process and bioH_2 conversion (Table 2 and Table 3).

In addition, the peak intensities at 1250 cm^{-1} (assigned to hemicellulose), 1160 cm^{-1} (related to carbohydrates) and 1060 cm^{-1} (assigned to cellulose) were weakened for *Thalia dealbata* but strengthened for *Phragmites* (sp.), suggesting the greater destruction in lignocellulosic structures of *Thalia dealbata* occurred by SE pretreatment. Furthermore, the fast decreased in values of both LOI and TCI by SE-[Bmim]Cl indicated the occurrence of greater disruption of cellulose crystallinity for *Thalia dealbata*. Therefore the increased amorphous cellulose in [Bmim]Cl-regenerated *Thalia dealbata* led to a better performance of enzymatic hydrolysis, [37, 41] resulting in bioH_2 conversion with high yield (Table 3).

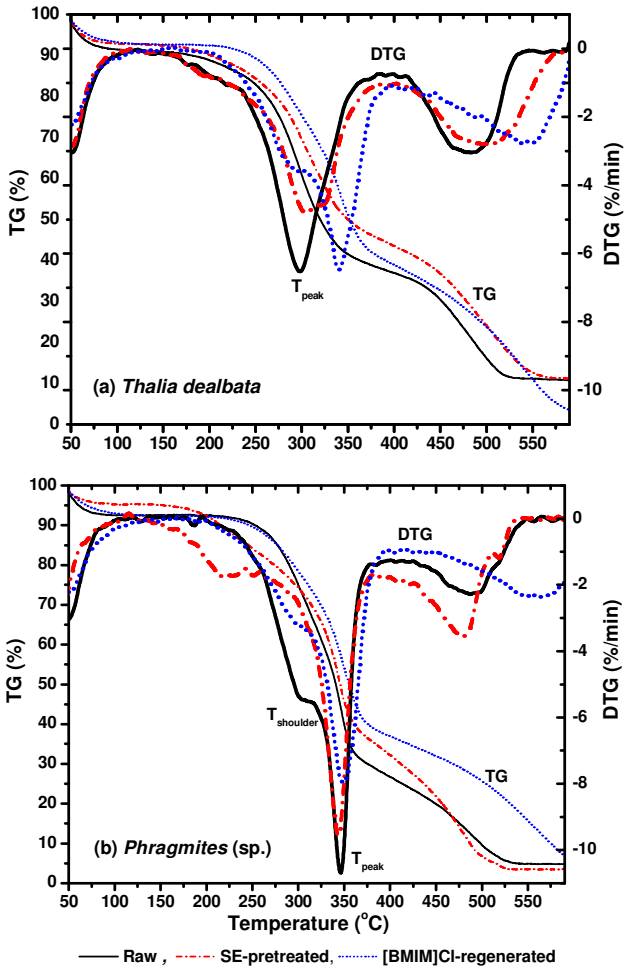

Fig. 10 TG/DTG curves of (a) *Thalia dealbata* (raw, SE-pretreated and [Bmim]Cl-regenerated *Thalia dealbata* (2.5MPa, 90s)) and (b) *Phragmites* (sp.) (raw, SE-pretreated and [Bmim]Cl-regenerated *Phragmites* (sp.) (3.0MPa, 90s)).

TG/DTG Curves. Regarding the differences of lignocellulosic components between *Phragmites* (sp.) and *Thalia dealbata,* measurements of TG/DTG were performed. In general, the thermal decomposition of hemicelluloses and cellulose appeared at temperatures in the range of 150 ~ 350 °C and 275 ~ 350°C, respectively, while lignin was featured by gradual decomposition at the temperatures ranging from 250 to 500 °C. [43] TG/DTG demonstrated in this study three distinct stages of weight loss for lignocellulosic substrates during thermal

decomposition (Fig. 10a and Fig. 10b). The first stage *ca*. 50 ~ 110 °C (dehydration); the second one *ca*. 140 ~ 410 °C, characteristic of hemicellulose decomposition appeared as a "shoulder" ($T_{shoulder}$) due to temperature intervals of hemicellulose and cellulose decomposition partially overlapped each other, and then attainment of the maximum (T_{peak}) mainly indicative of cellulose decomposition; the last stage *ca*. 410 ~ 550 °C, decomposition of lignin occurred in a wide range that overlaps partially with those of hemicelluloses and cellulose. [43-45]

The raw *Phragmites* (sp.) lignocelluloses had a more clear-cut separation between $T_{shoulder}$ (300 °C, related to hemicelluloses) and T_{peak} (350 °C, related to cellulose) (Fig. 10). While the raw *Thalia dealbata* exhibited a wide peak at 300 °C stemming from the thermal decomposition of cellulose and the curve of hemicellulose was almost merged by that of cellulose, the similar behavior of lignocellulosic substrate was found in willow and wood. [43] As seen from the DTG curves (Fig. 10), the amount of both cellulose and hemicellulose in the raw *Thalia dealbata* was relatively smaller than those of the raw *Phragmites* (sp.), which was in good accordance with lignocellulosic components analysis (Table 1).

The degradation of *Phragmites* (sp.) occurred within a narrower range of temperatures (T_{peak}) than that of *Thalia dealbata* even after pretreatments with SE and SE-[Bmim]Cl. This was mainly caused by the different sorts of hemicelluloses components and crystalline structures of cellulose as well as their variable distributions in plant species. [45] No big changes occurred in T_{peak} of *Phragmites* (sp.) after pretreatments with SE and SE-[Bmim]Cl. In contrast, SE-pretreatment shifted T_{peak} of *Thalia dealbata* towards higher T (305 - 325 °C), further higher T_{peak} (338 °C) was reached by SE-[Bmim]Cl treatment (Fig. 8a). This could come from the increased cellulose contents through removal of hemicelluloses as a consequence of SE pretreatment, while SE-[Bmim]Cl treatment increased amorphous cellulose components, thus increasing solid thermostability. The enhanced thermal stability of SE-[Bmim]Cl pretreated biomass appeared at higher temperatures was in agreement with the results from Labbe et al [46] and Singh et al. [47] In addition, the similar TG/DTG pattern occurred in regenerated materials of both plants after SE-[Bmim]Cl treatment, with T_{peak} around 338°C for *Thalia dealbata* and 350°C for *Phragmites* (sp.). This could be indicative of cellulose molecules of different polymerization degree, suggesting that higher polymerization degree of cellulose were in regenerated materials of *Phragmites* (sp.) than *Thalia dealbata*.

The presence of lignin was one of the most important factors affecting biotranformation of lignocellulosic substrates into $bioH_2$. A broad peak ranged from 410 to 550 °C mainly corresponded to lignin which overlapped partially with those of hemicelluloses and cellulose. SE-pretreatment changed intensities of this wide peak and it was shifted towards higher T at 530 °C for *Thalia dealbata* but towards lower T at 485°C for *Phragmites* (sp.) (Fig. 10). This could be related to the formation of different thermolabile chemical bonds in lignin fractionation as a consequence of SE. Further higher T above 550 °C was reached for both plants as a consequence of SE-[Bmim]Cl (Fig. 10). The alteration of lignin structure occurred in [Bmim]Cl-regenerated materials which could be attributed to the partially dissolution of lignin components in [Bmim]Cl (delignification). However, the structures and compositions of lignin in lignocellulosic substrates of both plants need be further elucidated before and after treatments. Furthermore, the combined [Bmim]Cl filtrates after use were concentrated and the regenerated [Bmim]Cl solvent was measured for the mass. The recovery rate of regenerated [Bmim]Cl solvent was as high as 91%, so that it can be reused for the dissolution of lignocellulosic substrates during $bioH_2$ transformation. Future investigation will focus on more structural elucidation of lignin components in regenerated [Bmim]Cl solvent in order to produce high value products of phenol compounds.

Conclusions

Compared to *Thalia dealbata*, *Phragmites* (sp.) displayed higher levels of cellulose and hemicellulose in substrate with high polymerization degree of cellulose, but possessed the lower surface area and pores volume of cellulose. Pretreatments with SE and SE-[Bmim]Cl were performed on the lignocellulosic substrate of both wetland plants. The optimal cellulose-rich fractionation of *Phragmites* (sp.) lignocelluloses yielded as a consequence of SE pretreatment under steam pressure at 3.0 MPa, while for *Thalia dealbata* lignocelluloses it was under steam pressure at 2.5 MPa. Compared to *Phragmites* (sp.), SE pretreatment greatly destroyed lignocellulosic structure of *Thalia dealbata* through hemicelluloses removal, thus increasing the accessible surface area and pores volume of cellulose in substrate. Furthermore, pretreatment with SE-[Bmim]Cl on lignocellulosic structure of plants effectively disrupted crystalline structure of cellulose or even solublize some lignin components, facilitating the formation of amorphous cellulose in regenerated materials with enhanced accessible surface area.

SE-[Bmim]Cl pretreatment led to lignocellulosic structures with improved properties efficient for their transformation into glucose and $bioH_2$ with elevated yields. Most importantly, higher $bioH_2$ conversion yielded from lignocelluloses of *Thalia dealbata* than *Phragmites* (sp.) possessing the denser lignocellulosic structure less efficient for $bioH_2$ conversion. To better understand the transformation of cell wall components into biofuel from wetland lignocellulosic substrates, further investigations will focus on more structural elucidation of hemicelluloses and lignin components in the products obtained from the pretreated samples as consequences of SE and SE-[Bmim]Cl treatments.

Experiment section

Materials

Lignocellulosic substrates used in this study were *Phragmites* (sp.) and *Thalia dealbata* from constructed wetlands located in Linan municipal wastewater treatment plant, Zhejiang Province, China. The harvested stalks of *Phragmites* (sp.) and *Thalia dealbata* at their maturities in early winter were naturally air dried, and then ground into 60 meshes using a cutting milling Restch, SM 100. The components of cellulose, hemicelluloses and lignin in stalks were evaluated according to the procedures from Van Soest. [48] Lignocellulosic substrates were dried at 60°C for 48 h and kept under vacuum for use.

2N NaOH aqueous solution was prepared from NaOH pellets (of analytical grade purity), 4 M HCl aqueous solutions was prepared from 37% (w/w) HCl (of analytical grade purity). 1-butyl-3-methyl-imidazolium chloride ([Bmim]Cl) (>95.0 % purity) was purchased from Shanghai Chengjie Chemical Reagent Ltd., China. Prior to use, [Bmim]Cl was dried under vacuum (0.1 Pa) at 70 °C (i.e. above the melting point) for at least 24 h to remove water completely.

Enzymatic hydrolysis was performed using 50 mM citric acid-sodium citrate buffer (pH 4.8), which was prepared from citric acid monohydrate (of analytical grade purity) and trisodium citrate (of analytical grade purity). Commercial enzyme Cellulase (activity 100 FPU/g) was purchased from Wuxi Xuemei Ltd., China. 3,5-Dinitrosalicylic acid (of analytical grade purity) was purchased from Aladdin (Shanghai) Reagent Ltd., China. D-Glucose, D-xylose, and cellobiose were of spectroscopic grade purities purchased from Aladdin (Shanghai) Reagent Ltd., China. Acetonitrile of HPLC grade purity was supplied by Sigma-Aldrich Co. FTIR samples were prepared with KBr (> 99.0% trace metal basis) was purchased from Sigma-Aldrich Co.

Pretreatment of Lignocellulosic Substrate with SE

Steam explosion (SE) pretreatment was performed on a QBS-80 batch steam explosion apparatus (Hebi Gentle Bioenergy Co. Ltd., China) which consisted of a high pressure vessel, a steam generator, a material tank, a receiver and a rapid-opening ball valve. The capacity of vessel was 400 mL with a maximum operating pressure of 4.0 MPa. The ground stalk lignocelluloses (~120 g) of *Phragmites* (sp.) or *Thalia dealbata* were subjected to the saturated steam in the vessel of each batch in apparatus, at ratio of water and lignocelluloses of 2:1 (ml/g). SE conditions were optimized by variation of saturated steam pressures (2.0, 2.5 and 3.0 MPa) and residence times for the pressure of saturated steam (60, 90 and 120 s) at the temperature of 230 °C. The pressure of saturated steam was maintained in high pressure vessel by the controller in apparatus at constant values of 2.0, 2.5 and 3.0 MPa, respectively, when changing residence time of saturated steam pressure in vessel. Then SE-fractionated lignocellulosic materials were recovered in the receiver and their components (cellulose, hemicelluloses and lignin) were measured following the method of Van Soest. [48] The raw and SE-pretreated lignocellulosic materials were dried at 60°C for at least 48 h and kept under vacuum for use.

Pretreatment of Lignocellulosic Substrate with SE-[Bmim]Cl

Microwave-assistant solubilisation in [Bmim]Cl solvent were performed on SE-pretreated lignocelluloses, which was optimized by changing ratios of lignocelluloses in [Bmim]Cl (varied from 1/5, 1/10, 1/20, 1/30 to 1/40 (w/w)), microwave power (among 80, 240, 400, 560 and 800W), and microwave heating time (among 28, 40, 52, 64 and 72 s). To obtain optimal microwave power, vacuum dried SE-pretreated lignocelluloses were mixed with vacuum dried [Bmim]Cl (at ratio of 1/20 (w/w)) in different vials, and then microwave power was given under 80, 240, 400, 560 and 800W, respectively, for 40s heating time. Then the optimal microwave heating time was achieved under the ratio of 1/20 (w/w) and 400 W microwave power, and the optimal ratio of lignocelluloses in [Bmim]Cl was obtianed under 400 W microwave power and 40s heating time.

Mixture of SE-pretreated lignocellulosic materials and [Bmim]Cl (at a 1/20 ratio) were used to perform the optimal microwave-assisted [Bmim]Cl dissolution condition (40s, 400W). [Bmim]Cl-regenerated materials were achieved by adding the sufficient deionized water as anti-solvents, centrifuged and dried at 60 °C for 48 h, then kept for enzymatic hydrolysis. Meanwhile, the components of cellulose, hemicelluloses and lignin in [Bmim]Cl-regenerated lignocelluloses were measured following the method of Van Soest. [48] Regarding the recovery of [Bmim]Cl after use, the combined [Bmim]Cl filtrates were concentrated by Rotary Evaporator (EYELA, Japan) under vacuum at 60 °C and finally freeze-dried under vacuum (0.1 Pa) at 70 °C for at least 48 h. The regenerated [Bmim]Cl was measured for the mass to yield recovery rate.

Enzymatic Hydrolysis

Saccharification hydrolysis occurred with 50 ml suspension of lignocellulosic substrates, using 10 ml of 50 mM citric acid-sodium citrate buffer (pH 4.8) and Cellulase levels from 2.5 to 50 FPU/g of dry substrates. After adding Cellulase, the vials were capped and placed in a HZ-9211KB rotary incubator (HUALIDA, China) at 50 °C and 180 rpm. One-milliliter sample was withdrew at specific time intervals, placed in a boiling (100°C) water bath for 15 min to deactivate the enzymes, and then centrifuged at ×1, 3000g (Fresco 17, Thermo, USA). A portion of 0.2 ml was used to measure the total reducing sugars by initrosalicylic acid (DNS) assay [49] with glucose, D-xylose and cellobiose (Aladdin) as standards. Residual filtrates were stored at -40 °C for subsequent sugar analyses by HPLC. Cellulase activity was determined by standard filter paper assay and expressed as filter paper units per gram (FPU). Hydrolysis rate of the reducing sugars from lignocellulosic materials was calculated as follows: Hydrolysis rate (%) = [(reducing sugars weight×0.9)/(dry lignocellulosic material weight × cellulose content)]×100.

BioH_2 Fermentation

Mixed anaerobic cultures used as the seed were obtained from anaerobic sludge digesters (as inoculum) at Linan municipal wastewater treatment plant, Zhejiang Province, China. The inoculum was first treated at 90 °C for 1 h to inhibit activity of methanogens and enrich in hydrogen producing bacteria. After lignocellulosic substrates were subjected to enzymatic hydrolysis for 24h, the hydrolysates in 60 ml obtained together with non-hydrolyzed solid fractions were initially introduced into each stoppered 150 ml serum bottle. Seed sludges (as inoculum) in 20 ml were also added to each bottle and batch thermophilic fermentation experiments were continuously conducted at 60 °C, with no additional nutrient medium solution. Initial pH was adjusted to 6.0 with 2 M NaOH or 4 M HCl. The headspaces of bottles were flushed with nitrogen gas to reach oxygen-free conditions. Procedures ended when pressure in bottle headspace started to drop off indicating hydrogen consumption. Biogas volume was monitored continuously with a water displacement method in the batch thermophilic fermentation experiments. Alkalified water was used to dissolve carbon dioxide and yield biogas.

Characterization

SEM images. Morphologies of raw and pretreated materials samples were observed with Scanning Electron Microscopy (SEM, HITACHI S-3400I, Japan) at an acceleration voltage of 5.0 kV, using samples sputter-coated with a thin layer of gold under vacuum condition before analysis.

Surface Area and Porosity Analyses. Accessible surface area and porosity of raw and pretreated materials samples were obtained from N_2 adsorption-desorption isotherms measured by an Automated Surface Area & Pore Size Analyzer (TriStarII, Micromeritics, USA), with samples evacuated at 50°C for 24 h under pressure of <0.25 Pa.

FTIR Spectra. Lignocellulosic structures of raw and pretreated materials samples were characterized. Fourier Transform Infrared (FTIR) spectra were recorded on a Bruker FTIR spectrophotometer (AVA TAR370, NICOLET, USA), ranging from 4000 to 400 cm^{-1} with the resolution of 4 cm^{-1} and 20 scans, using a KBr disc containing 1% finely ground samples.

TG/DTG Curve. A Pyris 1 TGA instruments (Perkin-Elmer, USA) was employed for the thermogravimetric tests on the raw and pretreated materials samples, with high-purity nitrogen used at flow rate of 150 ml/min. An inert was established before starting the heating program with the nitrogen purged for 20 min, then the experiments started with a drying session at a heating rate of 10 °C/min up to 600 °C and a holding time of 30 min.

HPLC Measurement. Glucose, xylose and cellobiose were quantified by HPLC (Shimadzu model LC-20A; Kyoto, Japan) equipped with a refractive index detector (RID 10A) and a styrene divinylbenzene resin column (ThermoHypersil-keystone NH2, 250 mm×4.6 mm, 5μm, UK) which was operated at 30 °C. The mobile phase consisted of 80% acetonitrile at a flow rate of 0.8 ml/min.

GC Measurement. The bioH_2 in biogas was analyzed using a GC9800 equipped with a thermal conductivity detector (TCD) and 6 feet stainless column which was packed with Porapak Q (80/100 mesh). The operational temperatures of the injection port, oven and TCD detector were maintained at 40, 80 and 60 °C, respectively. Nitrogen gas was used as the carrier at a flow rate of 20 ml/min.

Statistics

All statistical analyses were done in SigmaPlot (version 11). Two-way ANOVA with Tukey test post hoc procedure was employed to evaluate whether the means were significantly different at p=0.05.

Acknowledgements

This work was supported by grants from the Key Program for International Cooperation Project of the Ministry of Science and Technology of China (No. 2010DFB33960), Key Laboratory of Yangtze River Water Environment of Ministry of Education (Tongji University) of China (No. YRWEF201102), China Scholarship Council (No. 2011833072), and State Key Laboratory of Hydrology-Water Resources and Hydraulic Engineering, Nanjing Hydraulic Research Institute (No. 2013491311).

Notes and references

[a] *Key Laboratory of Environmental Remediation and Ecological Health, Ministry of Education, College of Environmental & Resource Sciences, Zhejiang University, Zijingang Campus, No. 866 Yuhangtang Rd, Hangzhou 310058, China*

[b] *College of Agriculture & Biotechnology, Zhejiang University, Zijingang Campus, No. 866 Yuhangtang Rd, Hangzhou 310058, China*

Fax: +86 571 86435070; Tel: +86 571 86435070

E-mail: penghongyun@zju.edu.cn

1 V. H. Smith, G. D. Tilman and J.C. Nekola, *Environ Pollut*, 1999, **100**, 179–196.
2 L.J. Sherwood and R.G. Qualls, *Environ Sci Technol*, 2001. **35**, 4126–4131.
3 H. Brix, *Water Sci Technol*, 1994. **30**, 209–223.
4 K. Abe and Y. Ozaki, 1998. *Soil Sci Plant Nutr*, **44**, 599–607.
5 C.H. House, B. A. Bergmann, A. M. Stomp, D. J. Frederick, *Ecol Eng*, 1999. **12**, 27–38.
6 L. L. Rectenwald and R.W. Drenner, *Environ Sci Technol*, 2000. **34**, 522–526.
7 D. Liu, X. Wu, J. Chang, B. J. Gu, Y. Min, Y. Ge, Y. Shi , H. Xue, C. H., Peng, J. G. Wu, *Nat Clim Chang*, 2012. **2**, 190–194.
8 M. R. Schmer, K. P. Vogel, R. B. Mitchell, R. K. Perrin, *Proc Natl Acad Sci USA*, 2008. **105**, 464–469.
9 N. Sathitsuksanoh, Z. G. Zhu, N. Templeton, J. A. Rollin, S. P. Harvey, Y-H. P. Zhang, *Ind Eng Chem Res*, 2009. **48**, 6441–6447.
10 F. L. Zhao, W. D. Yang, Z. Zeng, H. Li, X. E. Yang, Z. L. He, B. H. Gu, M. T. Rafiq, H.Y. Peng, *Biomass Bioenergy*, 2012. **42**, 212–218.
11 S. X. Zhu, H. L. Ge, Y. Ge, H. Q. Cao, D. Liu, J. Chang, C. B. Zhang, B. J. Gu, S. X. Chang, *Ecol Eng*, 2010. **36**,1307–1313.
12 H. Chen and M. M. Zhang, *Environ Sci Technol*, 2013, **47**, 8157–8163.
13 B. J. Gu, D. Liu, X. Wu,Y. Ge, Y. Min, H. Jiang, J. Chang, *Renew Sust Energ Rev*, 2011, **15**, 4910–4916.
14 C. L. Cheng, Y. C. Lo, K. S. Lee, D. J. Lee, C. Y. Lin, J. S. Chang, *Bioresour Technol*, 2011, **102**, 8514–8523.
15 D. Li and H. Chen, *Int J Hydrogen Energy*, 2007. **32**,1742–8.
16 R. Datara, J. Huanga, P. Manessa, A. Mohagheghia, S. Czernika, Chorn et al. R. Datar, J. Huang, P. C. Maness, A. Mohagheghi, S. Czemik, E. Chornet. *Int J Hydrogen Energy*, 2007. **32**, 932–939.
17 L. Ozkan, T. H. Erguder and G. N. Demirer, *Int J Hydrogen Energ*, 2011. **36**, 382–389.
18 M. Yoshida, Y. Liu, S. Uchida, K. Kawarada, Y. Ukagami, H. Ichinose, S. Kaneko, K. Fukuda, *Biosci Biotechnol Biochem*, 2008. **72**, 805–810.
19 F. Monlau, C. Sambusiti, A. Barakat, X. M. Guo, E. Latrille, E. Trably, J. P. Steyer, H. Carrere. *Environ Sci Technol*, 2012. **46**, 12217–12225.
20 F. Monlau, A. Barakat, E. Trably, C. Dumas, J. P. Steyer, H. Carrere. *Crit Rev Env Sci Tec*, 2013. **43**, 260–322.
21 J. E. Carrasco, C. M. C. Saiz, A. Navarro, P. Soriano, F. Saez, J. M. Martinez. *Appl Biochem Biotechnol*, 1994. **45/46**, 23–24.
22 J. B. Li, G. Gellerstedt and K. Toven. *Bioresour Technol*, 2009. **100**, 2556–2561.
23 A. P. Dadi, C. A. Schall and S. Varanasi, *Appl Biochem Biotechnol*, 2007. **137**, 407–421.
24 S. P. M. da Silva, A. M. D. Lopes, L. B. Roseiro, R. Bogel-Lukasik, *RSC Adv*, 2013. **3**, 16040–16050.
25 R. P. Swatloski, S. K. Spear, J. D. Holbrey, R. D. Rogers. *J Am Chem Soc*, 2002. **124**, 4974–4975.
26 I. Kilpeläinen, H. Xie, A. King, M. Granstrom, S. Heikkinen, D. S. Argyropoulos. *J Agric Food Chem*, 2007. **55**, 9142–9148.
27 S. H. Lee, T. V. Doherty, R. J. Linhardt, J. S. Dordick. *Biotechnol Bioeng*, 2009. **102**, 1368–1376.
28 C. L. Li, B. Knierim, C. Manisseri, R. Arora, H. V. Scheller, M. Auer, K. P. Vogel, B. A. Simmons, S. Singh. *Bioresour Technol*. 2010. **101**, 4900–4906.
29 M. G. Adsul, A. P. Terwadkar, A. J. Varma, D. V. Gokhale, *Bioresources*, 2009. **4**, 1670–1681.
30 J. S. Moulthrop, R. P. Swatloski, G. Moyna, R. D. Rogers, *Chem Commun*, 2005. 1557–1559.
31 T. Heinze, K. Schwikal, S. Barthel, *Macromol Biosci*, 2005. **5**, 520–

525.
32 A. Brandt, J. Grasvik, J. P. Hallett, T. Welton, *Green Chem*, 2013. **15**, 550–583.
33 M. E. Zakrzewska, E. Bogel-Lukasik, R. Bogel-Lukasik, *Energy Fuel*, 2010. **24**, 737−745.
34 A. Brandt, J. P. Hallett, D. J. Leak, R. J. Murphy, T. Welton, *Green Chem*, 2010. **12**, 672−679.
35 V. M. Egorov, S. V. Smirnova, A. A. Formanovsky, I. V. Pletnev, Y. A. Zolotov, *Anal Bioanal Chem,* 2007. **387,** 2263–2269.
36 A. M. D. Lopes, K. G. Joao, E. Bogel-Lukasik, L. B. Roseiro, R. Bogel-Lukasik, *J Agric Food Chem*, 2013. **61**, 7874–7882.
37 H. T. Tan, K. T. Lee, A. R. Mohamed, *Carbohyd Polym*, 2010. **83**, 1862–1868.
38 H. Zhao, C. I. L. Jones, G. A. Baker, S. Xia, O. Olubajo, V. N. Person. *J Biotechnol*, 2009. **139**, 47−54.
39 Y. Lu, Q. H. Lai, C. Zhang, H. X. Zhao, K. Ma, X. B. Zhao, H. Z. Chen, D. H. Liu, X. H. Xing. *Bioresour Technol*, 2009. **100**, 2889−2895.
40 I. Spiridon, C. A. Teaca and R. Bodirlau, *BioResources*, 2011, **6**, 400−413.
41 A. M. D. Lopes, K. G. Joao, D. F. Rubik, E. Bogel-Lukasik, L. C. Duarte, J. Andreaus, R. Bogel-Lukasik. *Bioresour Technol*, 2013. **142**, 198–208.
42 A. Carrillo, X. Colom, J. J. Sunol, J. Saurina, *Eur Polym J*, 2004. **40**, 2229–2234.
43 W. H. Chen, P. C. Kuo, *Energy*, 2010. **35**, 2580–2586.
44 V. I. Sharypov, N. Marin, N. G. Beregovtsova, S.V. Baryshnikov, B. N. Kuznetsov, V. L. Cebolla, J. V. Weber. *J Anal Appl Pyrol*, 2002. **64**,15−28.
45 J. M. Heikkinen, J. C. Hordijk, W. de Jong, H. Spliethoff, Thermogravimetry as a tool to classify waste components to be used for energy generation. *J anal appl pyrol*, 2004. **71**, 883−900.
46 N. Labbe, L. M. Kline, L. Moens, K. Kim, P. C. Kim, D. G. Hayes, *Bioresour Technol*, 2012. **104**, 701−707.
47 S. Singh, P. Varanasi, P. Singh, P. D. Adams, M. Auer, B. A. Simmons, *Biomass Bioenergy*, 2013. **54**, 276−283.
48 Van Soest. Van Soest fiber analysis. http://www.aquaculture.ugent.be/Education/coursematerial/online%20courses/ATA/analysis/vsoest.htm
49 G. L. Miller. *Anal Chem*, 1959. **31**, 426−428.